Available at
www.ElsevierComputerScience.com
POWERED BY SCIENCE DIRECT®

Signal Processing 85 (2005) 2137–2160

SIGNAL PROCESSING

www.elsevier.com/locate/sigpro

Comparison of linear signal processing techniques to infer directed interactions in multivariate neural systems

Matthias Winterhalder[a,b,*], Björn Schelter[a,b], Wolfram Hesse[c], Karin Schwab[c], Lutz Leistritz[c], Daniel Klan[c], Reinhard Bauer[d], Jens Timmer[a,b], Herbert Witte[c]

[a]*FDM, Freiburg Center for Data Analysis and Modeling, University of Freiburg, Eckerstr. 1, 79104 Freiburg, Germany*
[b]*Bernstein Center for Computational Neuroscience, University of Freiburg, Hansastr. 9, 79104 Freiburg, Germany*
[c]*Institute of Medical Statistics, Computer Sciences and Documentation, University of Jena, Bachstr. 18, 07743 Jena, Germany*
[d]*Institute of Pathophysiology and Pathobiochemistry, University Hospital of Jena, Nonnenplan 2, 07740 Jena Germany*

Available online 28 July 2005

Abstract

Over the last decades several techniques have been developed to analyze interactions in multivariate dynamic systems. These analysis techniques have been applied to empirical data recorded in various branches of research, ranging from economics to biomedical sciences. Investigations of interactions between different brain structures are of strong interest in neuroscience. The information contained in electromagnetic signals may be used to quantify the information transfer between those structures. When investigating such interactions, one has to face an inverse problem. Usually the distinct features and different conceptual properties of the underlying processes generating the empirical data and therefore the appropriate analysis technique are not known in advance. The performance of these methods has mainly been assessed on the basis of those model systems they have been developed for. To draw reliable conclusions upon application to empirical time series, understanding the properties and performances of the time series analysis techniques is essential. To this aim, the performances of four representative *multivariate linear* signal processing techniques in the time and frequency domain have been investigated in this study. The partial cross-spectral analysis and three different quantities measuring Granger causality, i.e. a Granger causality index, partial directed coherence, and the directed transfer function are compared on the basis of different model systems. To capture distinct properties in the dynamics of brain neural networks, we have investigated multivariate linear, multivariate nonlinear as well as multivariate non-stationary model systems. In an application to neural data recorded by electrothalamography and electrocorticography from juvenile pigs under sedation, directed as well as time-varying interactions have been studied between thalamic and cortical brain structures. The time-dependent alterations in local activity and changes in the interactions have been analyzed by the Granger causality index and the partial directed coherence. Both methods have been shown to be most

*Corresponding author. Tel.: +49 761 203 7710; fax: +49 761 203 7700.
E-mail address: matthias.winterhalder@fdm.uni-freiburg.de (M. Winterhalder).

0165-1684/$ - see front matter
doi:10.1016/j.sigpro.2005.07.011

suitable for this application to brain neural networks based on our model systems investigated. The results of this investigation contribute to the long-term goal to understand the relationships in neural structures in an abnormal state of deep sedation.

Keywords: Multivariate time series analysis; Granger causality; Cross-spectral analysis; Graphical models; Directed transfer function; Partial directed coherence

1. Introduction

Investigating the interrelations in the dynamics between different brain structures and synchronization phenomena between neural populations presents an important primary step toward the overall aim: the determination of mechanisms underlying pathophysiological diseases, primarily in order to improve treatment strategies especially for severe diseases. Synchronization phenomena or interrelations between different neural circuits have been observed e.g. in electroencephalography (EEG) data recorded during sedation or deep anesthetization. The detection, analysis, and monitoring of clinical EEG burst suppression patterns (BSP) during sedation or anesthesia are important because BSP can be seen as a defined reference point within the stream of changes in EEG characteristics during cerebro-protective treatment, i.e. sedation [1], or as a sign of unnecessary deep anesthesia [2].

BSP are characterized by alternating periods of high-voltage polymorphic activity, i.e. burst, and periods of nearly total amplitude-depression, i.e. suppression. A burst pattern consists of two main transient components, the delta-wave activity at 1–4 Hz and a delayed spindle oscillation within a higher frequency range of 7–16 Hz. Both are triggered by the burst onset. Burst duration is about 2–4 s. Steriade et al. [3,4] investigated the pacemakers of both components recorded by the electrocorticogram (ECoG) combined with intracellular recordings in the thalamus. They postulated that a disconnection between the thalamus and the cortex occurs during the suppression period and that burst periods appear after volleys from thalamocortical neurons. After the burst onset both delta wave and spindle oscillations are generated by the coordination of neural networks. The delta wave is the intrinsic rhythm of thalamocortical neurons and the delayed spindle oscillation is generated by thalamo-cortico-thalamic circuits. These generator structures can be investigated by electrocortico- and electrothalamographic recordings in animal experiments. As this cortical information transfer process is a time-variant structure, time-variant quantities are the most preferable. New time-variant methods for the quantification of neural information transfer are desired. Indeed, such model-related time-variant methods have been introduced successfully for burst pattern analysis [5–7]. Previously, for the quantification of information transfer between thalamic and cortical structures, correlation and coherence-based methods were used [8,9].

Analysis techniques based on correlation or coherence are not sufficient to adequately describe the interdependence within the neural system, such as the thalamo-cortico-thalamic circuits. As an example, assume that three signals are recorded in distinct brain structures, two signals from the thalamus and one signal from the cortex. If interrelations were investigated by an application of a bivariate analysis technique to each pair of signals and if a relationship was detected between both thalamic signals, they would not be necessarily directly linked. The interdependence between both thalamic signals might also be mediated by the cortical signal. To enable a differentiation between direct and indirect influences in multivariate systems, graphical models applying partial coherence have been introduced [10].

Beside detecting simple correlations between two signals in a multivariate network of processes, an uncovering of directed interactions enables deeper insight into the basic mechanisms underlying such networks. In our example of the thalamo-cortical network, it would be possible to

decide whether or not the thalamic leads project their information to the cortex or vice-versa. In some cases both directions might be present, possibly in distinct frequency bands. Granger [11] introduced a concept of causality based on the common sense idea that a cause must precede its effect, which allows inferring directed interactions in multivariate systems. Introducing the concept of Granger causality to multivariate analysis techniques, e.g. by the directed transfer function (DTF) [12], by the partial directed coherence (PDC) [13], or by a direct measure for Granger causality in the time-domain [14], has made these ideas more accessible for the analysis of coordination in brain neural networks. However, applying a single analysis technique to neural data without knowing its specific properties might yield misleading results. A comparison of the advantages and disadvantages of different analysis techniques is therefore desirable.

To this aim we investigate four multivariate signal processing techniques developed in the field of linear transfer function systems. The four analysis techniques originate from two classes, the class of non-parametric and the class of parametric analysis techniques. Representative of the non-parametric multivariate analysis technique, partial coherence (PC) and its corresponding partial phase spectrum is investigated. It has been used to reveal mainly undirected interactions in multivariate systems, such as tremor [15], neural system [16–18], or pollution data [10]. Other widely used analysis techniques such as quantities measuring phase or lag synchronization [19–22] have no multivariate extension that allows one to distinguish between direct and indirect interactions; a pairwise bivariate analysis is not sufficient to reveal the structure in multivariate networks. Multivariate cross-correlation analysis is not used because its information is already contained in its frequency counterpart, namely partial coherence [16,17]. Multivariate mutual information [23] is based on density estimation which is numerically difficult in multi-dimensional systems. Therefore these analysis techniques are not investigated in the present study. The class of parametric techniques is represented by a Granger causality index (GCI), the directed transfer function (DTF), and the PDC. These methods were applied in various fields of brain research [12–14,24–28,34].

The analysis techniques investigated here are characterized by different conceptual properties and reveal different dynamic effects such as nonlinearities in multivariate systems. Additionally, the ability to handle non-stationary signals is different between these methods. However, in applications to brain neural networks quantified for instance by EEG, the underlying dynamic is essentially unknown. Thus, requirements for the signal processing method applied are not obvious. For instance, neither nonlinearities nor non-stationarities of the neural signals should lead to an immediate breakdown of the method. To draw reliable conclusions in applications, one should be aware of the distinct features and the different performances of these analysis techniques. To this aim, all techniques are examined on the basis of simulated data with known dynamics first. Reliable conclusions about their performances are thus possible, since the true interaction structure is known in these systems. Furthermore, these model systems may serve as representatives for a large number of empirical neural networks.

We investigate synthetic signals simulated by different multivariate model systems with respect to five aspects: First, a differentiation between direct and indirect interrelations is examined. Second, a detection of the direction of interrelations is investigated. Third, the absence of any influence between the processes reflects the specificity of the methods. Fourth, since in many applications to brain neural networks the signals are at least weakly nonlinear, it is tested to which extent these analysis techniques can cope with nonlinearities. Fifth, time-varying dynamic effects are analyzed to investigate their performance on non-stationary data.

PDC is the analysis technique showing the best performance in revealing the multivariate interaction structure in the simulated model examples. Results from the DTF analysis are included in the results of the PDC analysis. The GCI is particularly useful if information in the time-domain is of special interest. Partial coherence as a non-parametric technique is shown to be robust in applications, because e.g. pre-knowledge of pro-

cess orders is not necessary. However, a time-variant partial coherence is not easily accessible.

Finally, we examine neural data recorded from juvenile pigs under sedation. Directed as well as time-varying interrelations are analyzed between the thalamic and cortical brain structures by PDC and the GCI. PDC yields a general overview over influences dependent on time and frequency, while the GCI is used to analyze the BSP more closely.

2. Multivariate linear time series analysis techniques

In this section, we summarize the theory of the multivariate linear time series analysis techniques under investigation, i.e. PC and partial phase spectrum (Section 2.1.1), the GCI (Section 2.2.1), the PDC (Section 2.2.2), and the DTF (Section 2.2.3). Finally, we briefly introduce the concept of directed graphical models (Section 2.3).

2.1. Non-parametric approaches

2.1.1. Partial coherence and partial phase spectrum

In multivariate dynamic systems, more than two processes are observed and a differentiation of direct and indirect interactions between the processes is desired. For this purpose bivariate coherence analysis is extended to partial coherence. The basic idea is to subtract linear influences from all other processes under consideration in order to detect directly interacting processes. The partial cross-spectrum

$$S_{XY|Z}(\omega) = S_{XY}(\omega) - S_{XZ}(\omega)S_{ZZ}^{-1}(\omega)S_{ZY}(\omega) \quad (1)$$

is defined between process X and process Y, given all the linear information of the remaining processes Z. Using this procedure the linear information of the remaining processes is subtracted optimally. Partial coherence

$$\mathrm{Coh}_{XY|Z}(\omega) = \frac{|S_{XY|Z}(\omega)|}{\sqrt{S_{XX|Z}(\omega)S_{YY|Z}(\omega)}} \in [0,1] \quad (2)$$

is the normalized absolute value of the partial cross-spectrum while the partial phase spectrum $\Phi_{XY|Z}(\omega) = \arg\{S_{XY|Z}(\omega)\}$ is its argument [8,10]. To test the significance of coherence values, critical values

$$s = \sqrt{1 - \alpha^{(2/v-2\,L-2)}} \quad (3)$$

for a significance level α depending on the dimension L of Z are calculated [35]. The equivalent number of degrees of freedom v depends on the estimation procedure for the auto- and cross-spectra. If for instance the spectra are estimated by smoothing the periodograms, the equivalent number of degrees of freedom [36]

$$v = \frac{2}{\sum_{i=-h}^{h} u^2(\omega_i)}, \quad \text{with} \sum_{i=-h}^{h} u(\omega_i) = 1 \quad (4)$$

is a function of the width $2h+1$ of the normalized smoothing window $u(\omega)$ evaluated at the harmonic frequencies ω_i.

Time delays and therefore the direction of influences can be inferred by evaluating the phase spectrum. A linear phase relation $\Phi_{XY|Z}(\omega) = d\omega$ indicates a time delay d between process X and process Y. The asymptotic variance

$$\mathrm{var}\{\Phi_{XY|Z}(\omega)\} = \frac{1}{v}\left[\frac{1}{\mathrm{Coh}^2_{XY|Z}(\omega)} - 1\right] \quad (5)$$

for the phase $\Phi_{XY|Z}(\omega)$ again depends on the equivalent number of degrees of freedom v (cf. Eq. (4)) and the coherence value at frequency ω [36]. The variance and therefore the corresponding confidence interval increases with decreasing coherence values. Large errors for every single frequency prevent a reliable estimation of the phase spectrum for corresponding coherence values which are smaller than the critical value s (cf. Eq. (3)). For signals in a narrow frequency band, a linear phase relationship is thus difficult to detect. Moreover, if the two processes considered were mutually influencing each other, no simple procedure exists to detect the mutual interaction by means of one single phase spectrum especially for influences in similar frequency bands.

2.2. Parametric approaches

Besides the non-parametric spectral concept introduced in the previous section, we investigate three parametric approaches to detect the direction

of interactions in multivariate systems. The general concept underlying these parametric methods is the notion of causality introduced by Granger [11]. This causality principle is based on the common sense idea, that a cause must precede its effect. For dynamic systems a process X is said to Granger-cause a process Y, if knowledge of the past of process X improves the prediction of the process Y compared to the knowledge of the past of process Y alone. Commonly, Granger causality is estimated by means of vector autoregressive models. Since a vector autoregressive process is linear by construction, only linear Granger causality can be inferred by this methodology. In the following, we will use the notion causality in terms of linear Granger causality.

The parametric analysis techniques introduced in the following are based on modeling the multivariate system by stationary n-dimensional vector autoregressive processes of order p (VAR[p])

$$\begin{pmatrix} X_1(t) \\ \vdots \\ X_n(t) \end{pmatrix} = \sum_{r=1}^{p} a_r \begin{pmatrix} X_1(t-r) \\ \vdots \\ X_n(t-r) \end{pmatrix} + \begin{pmatrix} \varepsilon_1(t) \\ \vdots \\ \varepsilon_n(t) \end{pmatrix}. \quad (6)$$

The estimated coefficient matrix elements $\hat{a}_{kl,r}$ $(k,l = 1,\ldots,n; r = 1,\ldots,p)$ themselves or their frequency domain representation

$$\hat{A}_{kl}(\omega) = \delta_{kl} - \sum_{r=1}^{p} \hat{a}_{kl,r}\, \mathrm{e}^{-i\omega r} \quad (7)$$

with the Kronecker symbol ($\delta_{kl} = 1$, if $k = l$ else $\delta_{kl} = 0$) contain the information about the causal influences in the multivariate system. The coefficient matrices weight the information of the past of the entire multivariate system. The causal interactions between processes are modeled by the off-diagonal elements of the matrices. The influence of the history of an individual process on the present value is modeled by the diagonal elements.

The estimated covariance matrix $\hat{\Sigma}$ of the Gaussian distributed noise $\varepsilon(t) = (\varepsilon_1(t), \ldots, \varepsilon_n(t))'$ contains information about instantaneous interactions and therefore, strictly speaking, non-causal influences between processes. But changes in the diagonal elements of the covariance matrix, when fitted to the entire systems as well as the subsystems, can be utilized to investigate Granger-causal influences, since the estimated variance of the residuals $\varepsilon_i(t)$ reflects information that cannot be revealed by the past of the processes. Additionally, the diagonal elements of the covariance matrix will become necessary for DTF and PDC which will be discussed in Section 3.2.

2.2.1. Granger causality index

To introduce a GCI in the time-domain and to investigate directed influences from a component X_j to a component X_i of a n-dimensional system, n- and $(n-1)$-dimensional VAR-models for X_i are considered. First, the entire n-dimensional VAR-model is fitted to the n-dimensional system, leading to the residual variance $\hat{\Sigma}_{i,n}(t) = \mathrm{var}(\varepsilon_{i,n}(t))$ for X_i. Second, a $(n-1)$-dimensional VAR-model is fitted to a $(n-1)$-dimensional subsystem $\{X_k, k = 1,\ldots,n | k \neq j\}$ of the n-dimensional system, leading to the residual variance $\hat{\Sigma}_{i,n-1}(t) = \mathrm{var}(\varepsilon_{i,n-1}(t))$.

A time-varying GCI quantifying linear Granger causality is defined by [14]

$$\gamma_{i \leftarrow j}(t) = \ln\left(\frac{\hat{\Sigma}_{i,n-1}(t)}{\hat{\Sigma}_{i,n}(t)}\right). \quad (8)$$

Since the residual variance of the n-dimensional model is expected to be smaller than the residual variance of the smaller $(n-1)$-dimensional model, $\gamma_{i \leftarrow j}(t)$ is larger than or equal to zero. For a time-resolved extension of the GCI, a time-variant VAR-parameter estimation technique is utilized by means of the recursive least square algorithm RLS which is a special approach of adaptive filtering [30]. Consequently, a time-resolved detection of directed interactions between two processes X_i and X_j is possible in the time-domain.

In the present study, the time-varying GCI is the only analysis technique under investigation reflecting information about multivariate systems in the time-domain. Alternative time-domain analysis techniques, such as the widely used cross-correlation function, are characterized by the property that their multivariate extensions are commonly estimated by means of the frequency-domain analysis techniques based on estimating partial

auto- and cross-spectra. Furthermore, complex covariance structures between time lags and processes make a decision about statistically significant time lags obtained by cross-correlation analysis difficult [37].

2.2.2. Partial directed coherence

As a parametric approach in the frequency-domain, PDC has been introduced to detect causal relationships between processes in multivariate dynamic systems. PDC accounts for the entire multivariate system and renders a differentiation between direct and indirect influences possible. Based on the Fourier transformation of the coefficient matrices (cf. Eq. (7)), PDC [13]

$$\pi_{i\leftarrow j}(\omega)=\frac{|A_{ij}(\omega)|}{\sqrt{\sum_k |A_{kj}(\omega)|^2}} \tag{9}$$

between processes X_j and X_i is defined, where $|\cdot|$ is the absolute value of $(\cdot)$. Normalized between 0 and 1, a direct influence from process X_j to process X_i is inferred by a non-zero PDC $\pi_{i\leftarrow j}$. To test the statistical significance of non-zero PDC values in applications to finite time series, critical values are used [38]. Similarly to the GCI, a significant causal influence detected by PDC analysis has to be interpreted in terms of linear Granger causality [11]. In the following investigations, parameter matrices have been estimated by means of multivariate Yule-Walker equations.

2.2.3. Directed transfer function

The DTF is a frequency-domain analysis technique to detect directions of interactions and is again based on the Fourier transformation of the coefficient matrices (cf. Eq. (7)). The transfer function $H_{ij}(\omega)=A_{ij}^{-1}(\omega)$ leads to the definition of the DTF [12,13]

$$\delta_{i\leftarrow j}(\omega)=\frac{|H_{ij}(\omega)|^2}{\sum_l |H_{il}(\omega)|^2}. \tag{10}$$

The DTF is normalized in [0,1]. An interaction from process X_j to process X_i is detected if $\delta_{i\leftarrow j}(\omega)$ is unequal to zero. The normalization in the definition of the DTF and the PDC is a major difference between both analysis techniques [29]. In the following, parameter matrices have been estimated based on multivariate Yule-Walker equations.

We note, however, that for the three parametric approaches under investigation, values quantifying the directed influences cannot be identified with the strength of the interactions directly.

2.2.4. Time-resolved extension of parametric approaches

In order to detect non-stationary effects in the interrelation structure of the multivariate system, an extension of the parametric approaches is introduced. To this aim a time-resolved parameter estimation technique is utilized. The GCI has already been introduced as a time-resolved procedure applying the recursive least square algorithm [30]. An alternative method to estimate time-resolved parameters in VAR-models, which specifically considers the influence of observation noise in the multivariate system, is based on time-varying state space models (SSMs) [39,40]

$$\begin{aligned} B(t) &= B(t-1)+\eta(t),\\ X(t) &= B(t-1)X(t-1)+\varepsilon(t),\\ Y(t) &= C(t)X(t)+\tilde{\eta}(t). \end{aligned} \tag{11}$$

SSMs consist of hidden state equations $B(t)$ and $X(t)$ as well as an observation equation $Y(t)$. The hidden state equation for $B(t)$ includes the time-dependent parameter matrices $a_r(t)$ (compare with Eq. (6)). The observation equation $Y(t)$ explicitly takes account of observation noise $\tilde{\eta}(t)$. For a numerically efficient procedure to estimate the parameters in the SSM, the EM-algorithm based on the extended Kalman filter or for known variances and observation matrix the extended Kalman filter is used [41].

2.3. Directed graphical models

Graphical models are a methodology to visualize and reveal relationships in multivariate systems [42]. Such a graph is shown in Fig. 1. The vertices reflect the processes and the arrows the interactions between the processes detected by the analysis technique applied. For example, if PDC is only significant from process X_4 to process X_2 but not in the opposite direction, an arrow is

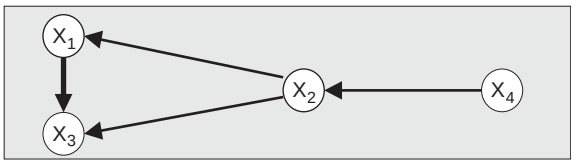

Fig. 1. Directed graph summarizing the interdependence structure for the VAR-model of example 1.

drawn from process X_4 to process X_2. In contrast, if PDCs are non-significant between process X_3 and process X_4, both processes are identified as not directly influencing each other and arrows between the processes in the corresponding graphical model are absent. In the following, dashed arrows will be drawn for specific properties of the corresponding analysis technique, for instance an indirect interaction between processes spuriously detected by the analysis technique applied.

3. Comparison of analysis techniques based on investigations of simulated, multivariate systems

The performance of the previously introduced multivariate linear time series analysis techniques is investigated by means of synthetic data simulated by different types of model systems. To illustrate the intrinsic differences between the analysis techniques, an investigation of a linear model system is given in Section 3.1. As discussed in Section 3.2, problems with parametric approaches may arise if independent processes with a wide difference in variance are observed. To investigate the capability of these methods to detect couplings in nonlinear multivariate systems, a coupled stochastic Roessler system is analyzed in Section 3.3. Finally, non-stationary effects are examined by means of a linear VAR-model with parameter changes dependent on time in Section 3.4.

3.1. Example 1: Four-dimensional vector autoregressive process

To show the properties of the four linear multivariate analysis techniques, a multivariate linear system has been investigated. Since all techniques are developed for such systems, a successful application is guaranteed. Therefore, the following example shows the intrinsic properties of the analysis technique and not properties related to the simulated processes. As a representative of the class of linear stochastic dynamic systems, a four-dimensional VAR[5]-process,

$$\begin{aligned} X_1(t) &= 0.8\,X_1(t-1) + 0.65\,X_2(t-4) + \eta_1(t),\\ X_2(t) &= 0.6\,X_2(t-1) + 0.6\,X_4(t-5) + \eta_2(t),\\ X_3(t) &= 0.5\,X_3(t-3) - 0.6\,X_1(t-1) + 0.4\,X_2(t-4)\\ &\quad + \eta_3(t),\\ X_4(t) &= 1.2\,X_4(t-1) - 0.7\,X_4(t-2) + \eta_4(t), \end{aligned} \quad (12)$$

has been examined. The covariance matrix of the noise terms $\eta_i(t)$ has been set to the identity matrix and $N = 50.000$ data points have been simulated. The simulated interdependence structure of the vector autoregressive process is summarized by the graph in Fig. 1.

The time-resolved values of the GCI are given in Fig. 2(a). The corresponding graph based on the analysis using the GCI is shown in Fig. 2(b) and is identical to the graph corresponding to the simulated VAR-model. The GCI detects all simulated interdependencies as well as the direction of the influences correctly. For instance, considering the influence from process X_1 to process X_2, the corresponding GCI fluctuates around zero. In contrast, by means of the GCI, the opposite influence from process X_2 to process X_1 is detected correctly.

In Fig. 2(c), partial coherences as well as partial phase spectra are shown. Critical values for a 5%-significance level for the partial coherence are shown by the gray lines. The corresponding graph based on this analysis is given in Fig. 2(d). The interdependence structure in the VAR-model is again detected correctly. Partial coherence analysis reveals indirect interrelations between processes X_1 and X_4 as well as between processes X_3 and X_4. By means of the partial phase spectra, directions of influences are inferred. For example, partial phase spectrum between processes X_1 and X_2 can be approximated by a linear phase relation with negative slope, correctly indicating an influence from processes X_2 to X_1. The phase relation between processes X_1 and X_3 is not linear, which

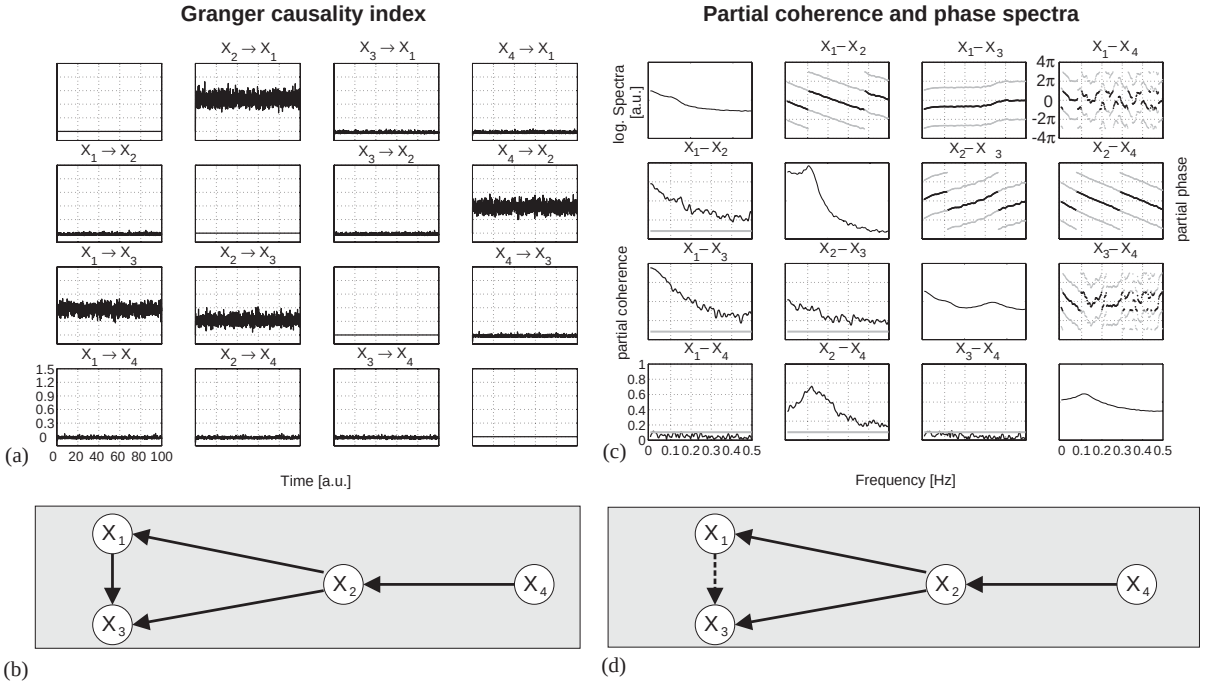

Fig. 2. Granger causality index for the VAR-model in example 1 (a) and resulting directed graph (b). The simulated interrelation structure is reproduced correctly by non-zero values of the Granger causality index. Partial coherence and corresponding phase spectra (c). Spectra are shown on the diagonal. Above the diagonal partial phase spectra and below the diagonal the partial coherences are shown. Two interrelations are unmasked as indirect ones by partial coherence. There is no direct mutual linear influence between the processes X_1 and X_4 and the processes X_3 and X_4. For these two influences the phase spectra are also not interpretable due to the low partial coherence values. Calculating the slopes of the phase spectra, time lags between processes can be estimated. The resulting graph is shown in (d). The dashed arrow indicates that there is no linear phase relationship between the processes X_1 and X_3.

is indicated by the dashed arrow in the graph in Fig. 2(d).

Results of an analysis using the DTF are given in Fig. 3(a) and the resulting graph in Fig. 3(b). By means of DTF analysis, all directions of interactions are detected correctly. Nevertheless, a differentiation between direct and indirect influences is impossible. This is illustrated by dashed arrows in the graph. Process X_4 is neither directly influencing process X_1 nor process X_3. Both influences are mediated by process X_2. In Fig. 3(c) PDC and in Fig. 3(d) the corresponding directed graph is given. In contrast to the DTF, PDC analysis differentiates between direct and indirect interactions and detects the corresponding directions of influences correctly. The graph resulting from PDC analysis is identical to the graph corresponding to the simulated VAR-model (cf. Fig. 1).

3.2. Example 2: Three independent white noise processes

In the previous section, we have demonstrated the intrinsic properties of the analysis techniques under investigation and their high sensitivity in detecting direct influences in multivariate systems. The following investigation was performed in order to test their reliability in the absence of any influence between the processes, reflecting the specificity of the methods in detecting influences. The variances of the processes, to be more precise the variance of the stochastic influence, differ substantially in the following example. In applications to neural signals, for instance by analyzing scalp or invasive EEG recordings, this situation may arise. The following investigation illustrates that a specific normalization procedure is required to avoid false detections of influences when

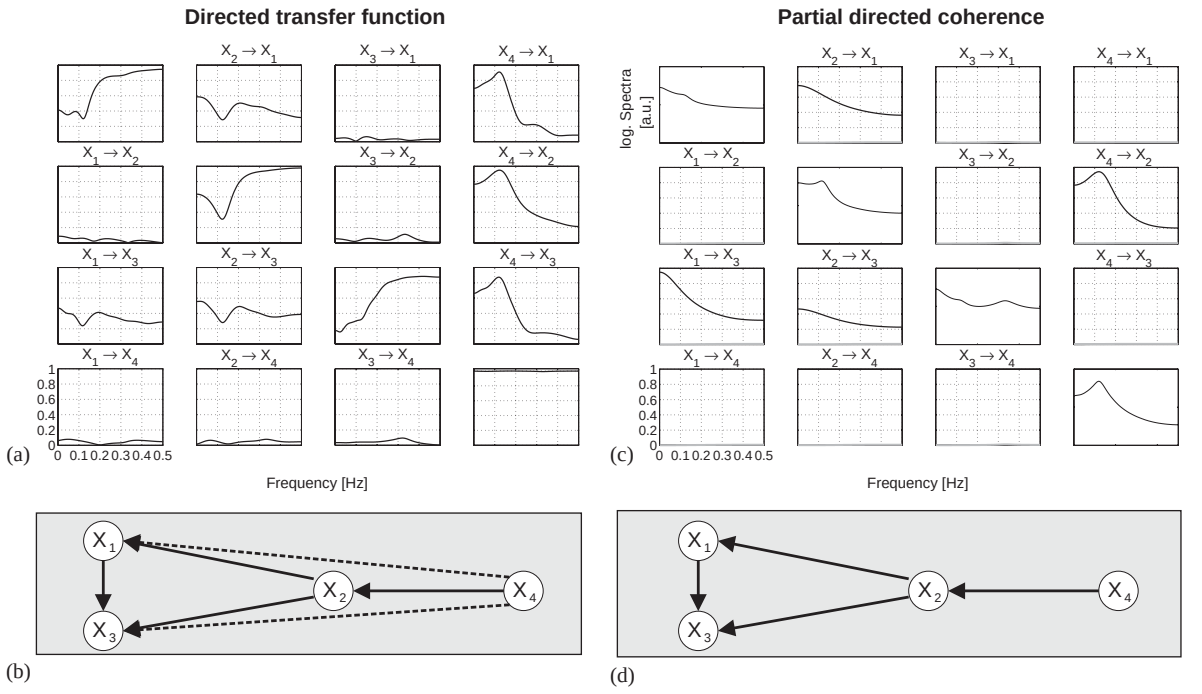

Fig. 3. Directed transfer function for the VAR-model of example 1 (a). The auto-directed transfer functions $\delta_{i\leftarrow i}$ are given on the diagonal. The directed interdependencies are summarized in the graph in (b). Besides the true interactions, two indirect influences are detected as directed ones by means of the directed transfer function, indicated by the dashed arrows. Partial directed coherence is given in (c) and the resulting graph in (d). The simulated interdependence structure has been reproduced correctly.

applying parametric approaches based on VAR-modeling of the system investigated. Thus, three *independent* white noise processes $X_1(t) = \sigma_1\eta_1(t)$, $X_2(t) = \sigma_2\eta_2(t)$, $X_3(t) = \sigma_3\eta_3(t)$, $\eta_i \sim N(0,1)$ have been simulated with 10.000 data points each and different variances $\sigma_{2,3} = 500 \cdot \sigma_1$. In Fig. 4(a) the values of the GCI is shown and in Fig. 4(b) the resulting graph. No Granger-causal influence between the three processes is indicated.

In Fig. 5 results for DTF (a) and PDC (b) are given. For this analysis an order of $p = 10$ for the fitted VAR-model has been chosen. When applying both techniques directly to the signals X_i, influences from process X_1 to process X_2 and to process X_3 are observed by DTF and PDC analysis (gray lines). This result is illustrated in the graph in Fig. 5(c) by dashed arrows.

False detection of influences is caused by the differences in the variance between X_1, X_2 and X_3, leading to spurious, directed influences from the process with low variance to the processes with significantly higher variances. The difference in the variance yields large errors on the parameter estimates. A renormalization of the covariance matrix $\hat{\Sigma}$ of the noise of the estimated VAR-model, such that the covariance matrix $\hat{\Sigma}$ of the estimated VAR-model approximately equals the identity matrix and subsequent application of the parametric analysis technique, leads to the correct results. This is shown in Fig. 5(a) and (b) by the black lines. No directed influences are indicated and the independence between the noise processes is reproduced correctly.

3.3. Example 3: Four-dimensional coupled stochastic Roessler system

An additional challenge expected in applications to time series representing neural signal transfer is a possible nonlinearity of the processes. At least weakly nonlinear dynamic systems must not lead immediately to wrong results when applying

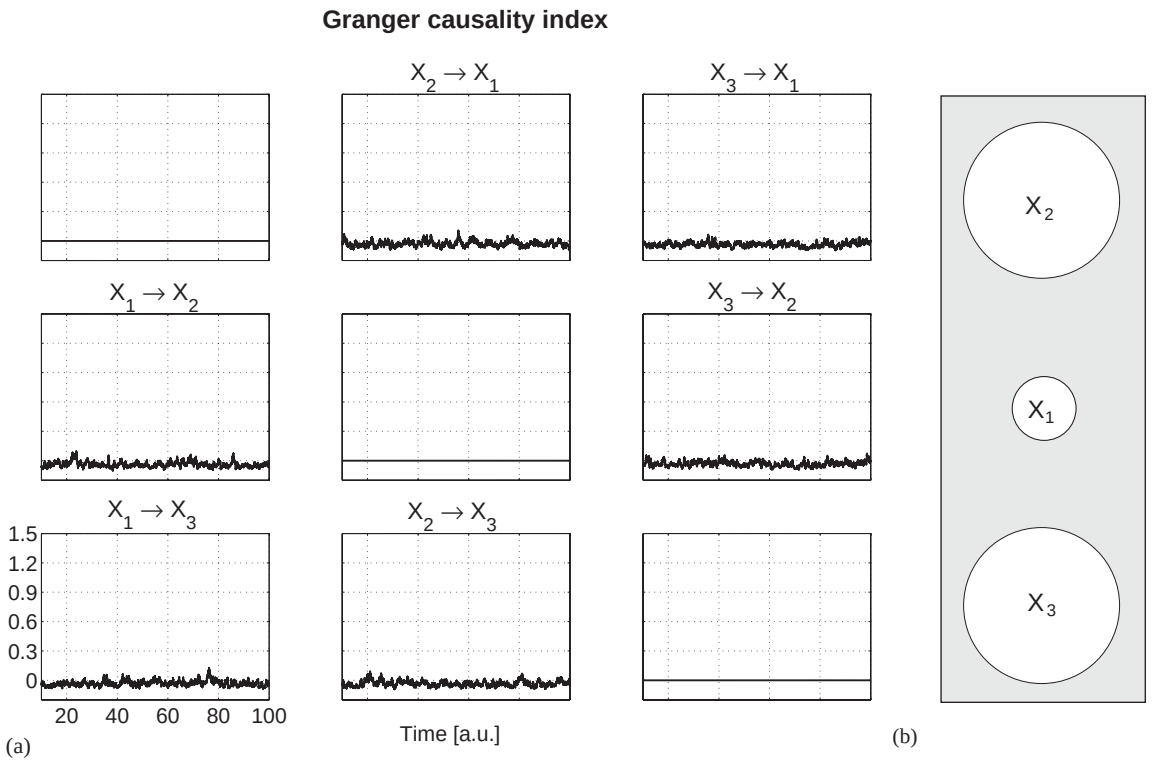

Fig. 4. Granger causality index for three independent white noise processes. Due to the estimation of the vector autoregressive model, values of the Granger causality index are missing for the first ten time units. In agreement with the simulation, no Granger-causal influence between the three independent processes is detected. The graph resulting from the Granger causality index is given in (b).

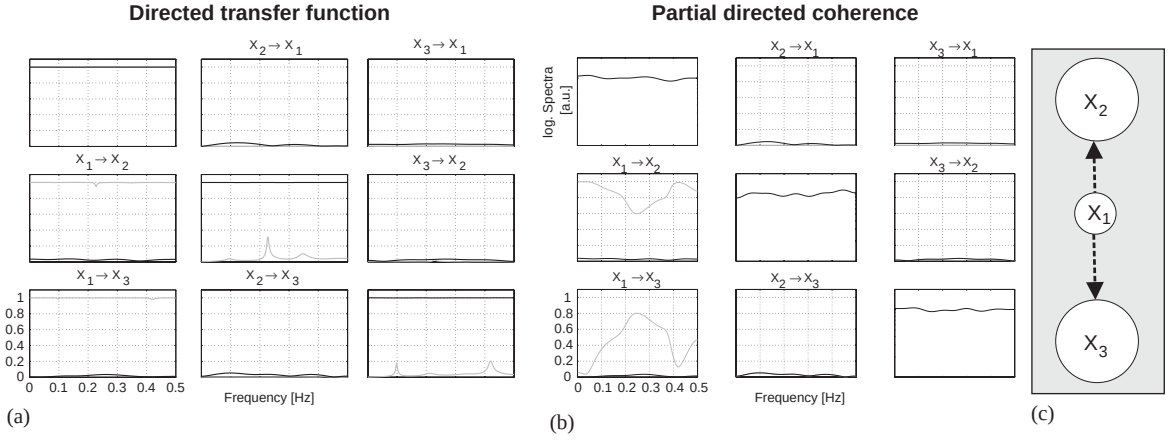

Fig. 5. Directed transfer function (a) and partial directed coherence (b) for the example of three independent white noise processes. Without preprocessing of the signals, a directed influence is detected from process X_1 onto the remaining two processes (gray lines). The graph summarizing the results is shown in (c). Dashed arrows indicate the spurious interactions. A renormalization of the estimated noise covariance matrix leads to correct results, illustrated by the black lines for both analysis techniques.

multivariate linear analysis techniques. To examine the performance of the linear methods in application to a nonlinear stochastic systems, a coupled stochastic Roessler system [33]

$$\begin{pmatrix} \dot{X}_j \\ \dot{Y}_j \\ \dot{Z}_j \end{pmatrix} = \begin{pmatrix} -\Omega_j Y_j - Z_j + \left[\sum_i \kappa_{ji}(X_i - X_j)\right] + \eta_j \\ \Omega_j X_j + a Y_j \\ b + (X_j - c) Z_j \end{pmatrix}$$
$$i,j = 1,2,3,4 \qquad (13)$$

with frequencies Ω_j has been analyzed. The frequencies of the four oscillators have been shifted using $\Omega_1 = 1.01$, $\Omega_2 = 0.99$, $\Omega_3 = 0.97$, and $\Omega_4 = 1.03$. The parameters of the oscillators have been set to $a = 0.15$, $b = 0.2$, and $c = 10$. The stochastic influence is given by Gaussian distributed white noise η_j. The interaction between oscillator i and oscillator j is modeled by means of a coupling between the X_i- and X_j-component and the coupling strength is adjusted by the coupling parameters $\kappa_{ji} \neq 0$. In the following, the coupling parameters have been set to $\kappa_{12} = 0.04$, $\kappa_{21} = 0.04$, $\kappa_{41} = 0.04$, $\kappa_{13} = 0.04$, $\kappa_{34} = 0.04$. The remaining couplings strengths have been set to zero. The simulated coupling scheme is summarized in the graph in Fig. 6. The nonlinear stochastic system has been simulated using an Euler method with an integration step of 0.004, a sampling step of 0.1, and $N = 50.000$ data points. The time series analysis techniques have been applied to X-components of the Roessler system in the following.

Applying the GCI to this nonlinear system, no directed relationship between any of the processes is detected (data not shown). Due to the high model order which is required to describe the nonlinear processes sufficiently well, higher fluctuations of the GCI are observed compared to the previous investigations of vector autoregressive models.

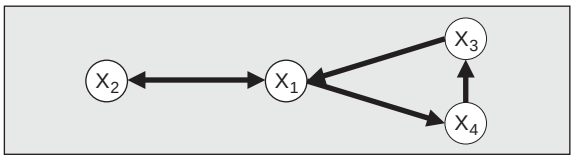

Fig. 6. Directed graph summarizing the coupling scheme of the coupled stochastic Roessler system.

For oscillatory processes with pronounced frequencies, analysis techniques in the frequency domain are preferable. In Fig. 7(a) results for the application of the DTF are shown and in (b) the resulting directed graph. The DTF is characterized by peaks at the oscillation frequencies $f_i = \Omega_i/2\pi \approx 0.16$ of the Roessler oscillators. For the DTF, no analytic significance level based on the statistical properties of this quantity has been derived so far. Surrogate data tests based on Fourier transformation and shuffling of phases have been proposed to estimate confidence levels [29]. While results obtained by this procedure might be true, we doubt the formal correctness of these confidence levels. For instance, shuffling the phases and inverse Fourier transformation leads to a stationary linear system of independent time series [43]. Tests for the absence of coupling might thus also test against stationarity or linearity of the system. Therefore, false positive conclusions about the presence of interactions are possible. Due to these problems related to surrogate data testing, we did not utilize this procedure in the present investigation.

Nevertheless, high values of the DTF at the oscillation frequencies are observed for the influence from process X_3 to process X_1 and from process X_4 to process X_3, indicated by solid arrows in the graph. Smaller directed influences are suggested in both directions between process X_1 and process X_2 as well as from process X_1 to process X_4, indicated by dashed arrows in the graph.

To illustrate a specific problem which might occur when analyzing multivariate dynamical systems, results for bivariate coherence analysis ($\mathrm{Coh}_{XY|Z=0}(\omega)$) are shown in addition to partial coherence analysis in Fig. 8(a). Critical values for a 5%-significance level are given by the gray lines. The resulting graph is given in Fig. 8(b). Due to the functional relationship of the asymptotic variance of the phase spectrum (cf. Section 2.1.1), directions of influences are not reliably detectable by means of partial phase spectra. Apart from bivariate coherence between processes

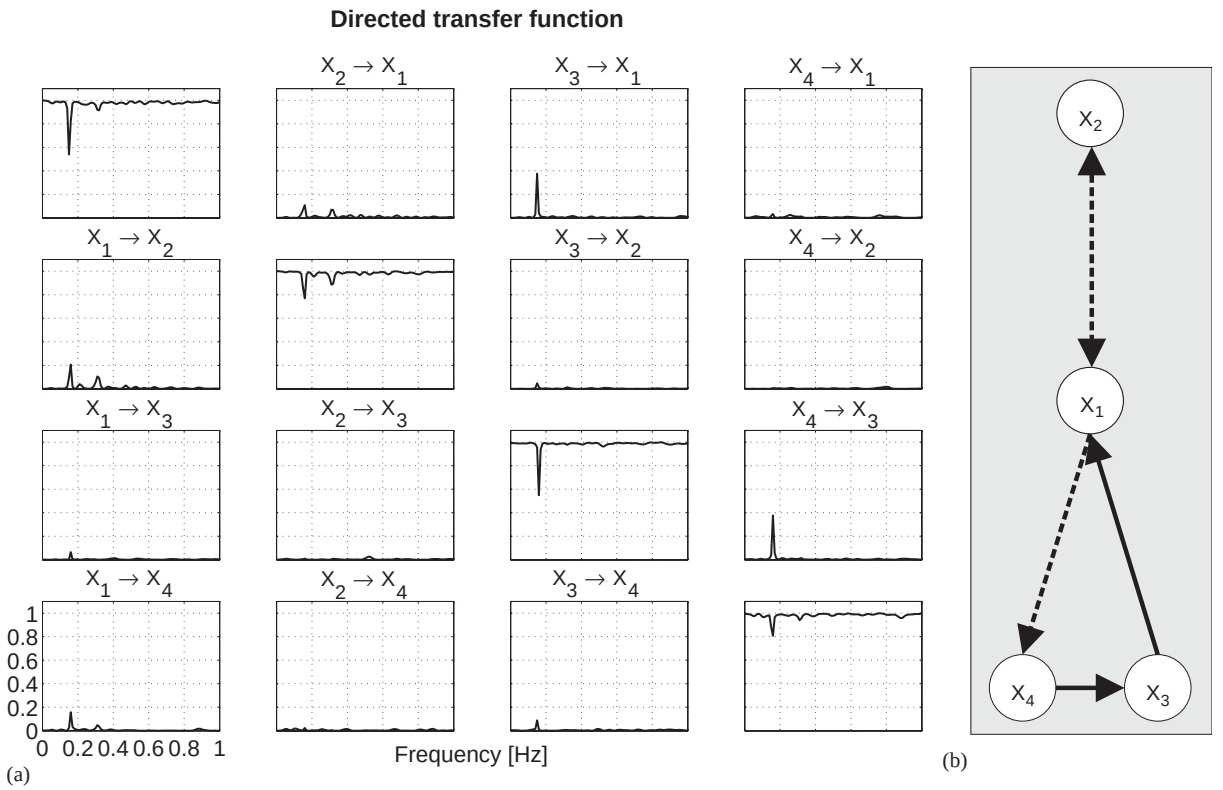

Fig. 7. Directed transfer function for the coupled stochastic Roessler system (a). The auto-directed transfer functions $\delta_{i\leftarrow i}$ are shown on the diagonal. Due to the absence of an analytic significance level, results are difficult to interpret in this example. However, higher values of the directed transfer function at the oscillation frequencies indicate the direction of the influences summarized in the graph in (b). Dashed arrows reflect low values of the directed transfer function.

X_2 and X_3, all bivariate coherences are significant at the oscillation frequency. The indirect coupling between the oscillators X_2 and X_4 is revealed correctly, as partial coherence is non-significant at the oscillation frequency. However, a significant partial coherence is observed between oscillators X_2 and X_3 although the bivariate coherence between both processes is non-significant. This effect is called *marrying parents of a joint child* and is explained as follows:

Both processes X_2 and X_3 influence process X_1 but do not influence each other. This is correctly indicated by bivariate coherence analysis between oscillator X_2 and oscillator X_3. In contrast to bivariate coherence, partial coherence between X_2 and X_3 conditions on X_1. To explain the significant partial coherence between the processes X_2 and X_3, the specific case $X_1 = X_2 + X_3$ is considered. A subtraction of the optimal linear information $1/2(X_2 + X_3)$ from X_2 leads to $1/2(X_2 - X_3)$. Analogously, a subtraction of the optimal linear information $1/2(X_2 + X_3)$ from X_3 leads to $-1/2(X_2 - X_3)$ (cf. Section 2.1.1). As coherence between $1/2(X_2 - X_3)$ and $-1/2(X_2 - X_3)$ is one, the partial coherence between X_2 and X_3 becomes significant. This effect is also observed for more complex functional relationships between process X_1 and the processes X_2 and X_3. The "parents" X_2 and X_3 are connected and "married by the common child" X_1. The interrelation between X_2 and X_3 is still indirect, even if the partial coherence is significant. In conclusion, the *marrying parents of a joint child* effect should not be identified as a direct interrelation between the

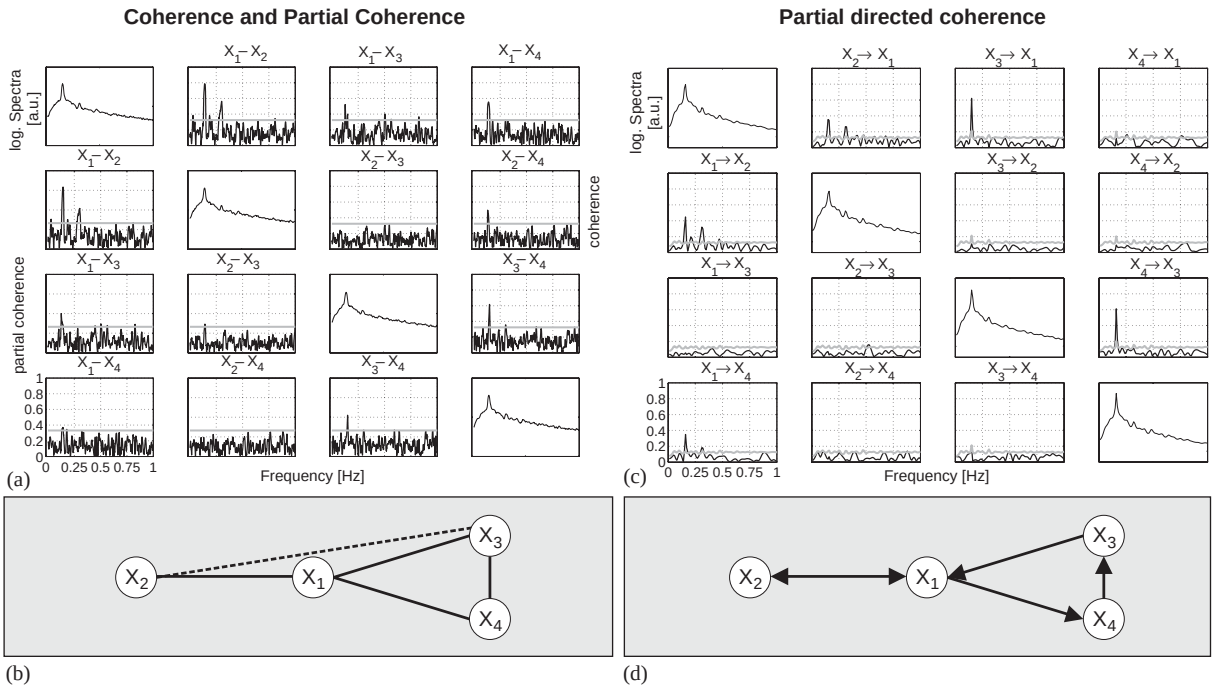

Fig. 8. Coherence and partial coherence for the coupled stochastic Roessler system (a). In the upper right corner bivariate coherences are shown. In the lower left corner, partial coherences are shown. The significance level is given by the gray line. On the diagonal the spectra of the processes are shown. Except from the coherence between processes X_2 and X_3, each pair of processes are bivariately coherent at the oscillation frequency. However, partial coherence analysis is significant between processes X_2 and X_3 at the oscillation frequency, indicating that there is a direct interrelation between both processes. This apparently contradicting result is illustrated by the dashed line in the undirected graph in (b). Results of partial directed coherence analysis (c). The level of significance is indicated by the gray lines. The resulting graph is given in (d) and the simulated coupling scheme is reproduced correctly.

corresponding processes and is detected by simultaneous calculation of bivariate coherence and partial coherence.

The coupling scheme within the Roessler system is detected correctly by PDC analysis using a sufficiently high order $p = 200$ for the VAR-model. PDC is shown in Fig. 8(c) and the resulting directed graph in Fig. 8(d). Critical values for a 5%-significance level are given by the gray lines. The bidirectional coupling between processes X_1 and X_2 as well as all unidirectional couplings are detected by significant PDC values at the oscillation frequency.

3.4. Example 4: Three-dimensional VAR-process with non-stationary parameters

The final investigation of synthetic data sets is devoted to non-stationary signals. For this purpose, analysis techniques revealing time-varying influences are required. When neglecting the presence of non-stationarities in neural data, averages of interactions in neural signal transfer would be estimated.

But changes in the interactions may contain the most relevant information, e.g. when analyzing EEG recordings of epilepsy patients in the transition to a seizure. For a focal epilepsy, a seizure starts from a well-defined area in the brain and spreads until large areas of the brain are involved in the seizure. Changes in interactions are taking place during seizure spread and are therefore of particular interest. A different example is the processing of sensory input. The temporal variations in the interaction might infer the way information is processed by the brain.

The application of the multivariate analysis techniques to non-stationary systems has been

examined in the following by a three-dimensional VAR [2]-process with time-varying parameters

$$\begin{aligned} X_1(t) &= a_1(t)X_1(t-1) + b_1(t)X_1(t-2) \\ &\quad + c_{12}(t)X_2(t-1) + c_{13}(t)X_3(t-1) + \eta_1(t), \\ X_2(t) &= a_2(t)X_2(t-1) + b_2(t)X_2(t-2) \\ &\quad + c_{21}(t)X_1(t-1) + c_{23}(t)X_3(t-1) + \eta_2(t), \\ X_3(t) &= a_3(t)X_3(t-1) + b_3(t)X_3(t-2) \\ &\quad + c_{31}(t)X_1(t-1) + c_{32}(t)X_2(t-1) + \eta_3(t), \\ \eta_i &\sim N(0,1), \quad i = 1,2,3. \end{aligned} \tag{14}$$

$N = 10.000$ data points have been simulated. The process parameters $a_1 = 0.5$, $a_2 = 0.7$, $a_3 = 0.8$, $b_1 = 0.7$, $b_2 = -0.5$, and $b_3 = 0$ have been kept constant. The influence from process X_2 to process X_1 was given by

$$c_{21}(t) = \begin{cases} 0.5\frac{t}{5.000} & \text{if } t \leqslant 5.000, \\ 0.5\frac{10.000-t}{5.000} & \text{else,} \end{cases} \tag{15}$$

modeling a positive triangular function with a maximum value of 0.5 in the middle of the simulation period. The influence in the opposite direction has been chosen to be constant at a value $c_{21}(t) = 0.2$. A unidirectional influence from process X_3 to X_2 was given by

$$c_{23}(t) = \begin{cases} 0.4 & \text{if } t \leqslant 7.000, \\ 0 & \text{else,} \end{cases} \tag{16}$$

modeling an abrupt breakdown of the influence after 70% of the simulation period. The remaining parameters modeling the influences have been set to zero, i.e. $c_{32}(t) = c_{13}(t) = c_{31}(t) = 0$. The simulated interdependence structure is summarized in Fig. 9.

Values of the GCI are given in Fig. 10(a) and the resulting graph in (b). The triangularly modulated influence from process X_2 to process X_1 is detected correctly as well as the abrupt change in the influence from process X_3 to process X_2. As the constant influence from process X_1 to process X_2 is rather weak, the GCI is only slightly different from zero. However, compared to the remaining values of the GCI, a direct influence from process X_1 to process X_2 is indicated (dashed arrow in the graph). The GCI is capable of reproducing the non-stationary interdependence structure.

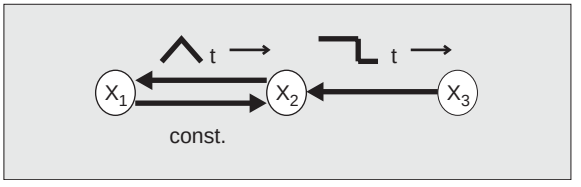

Fig. 9. Directed graph summarizing the interdependence structure of the VAR-model with non-stationary parameters.

In Fig. 11(a) the results for the DTF are shown and the resulting graph in Fig. 11(b). The auto-DTFs of the processes are shown on the diagonal. Apart from one spurious influence from process X_3 to process X_1, indicated by the dashed arrow, all influences and their changes are detected correctly by means of DTF analysis. Results for application of PDC based on state space modeling and the resulting graph are given in Fig. 11(c) and (d), respectively. The spectra of the three processes are shown on the diagonal. The spurious directed influence from process X_2 to X_3 during the first few time points is caused by edge effects of the estimation procedure. Small PDC values for the influence from process X_1 and process X_2 to process X_3 are considered to be negligible. The remaining influences, their directions as well as their non-stationary behavior are reproduced correctly using PDC.

4. Application to neural data

In order to examine time-variant causal influences within distinct neural networks during defined functional states of brain activity, data obtained from an experimental approach of deep sedation were analyzed. BSP in the brain electric activity were used for the analysis. This specific functional state was chosen because BSP represent a defined reference point within the stream of changes in EEG properties during sedation [1] leading to secured unconsciousness. An analysis of well-described alternating functional states of assumed differences of signal transfer in a time frame of seconds is possible. It has been shown that a hyperpolarization block of thalamo-cortical neurons evoked mainly by facilitated inhibitory

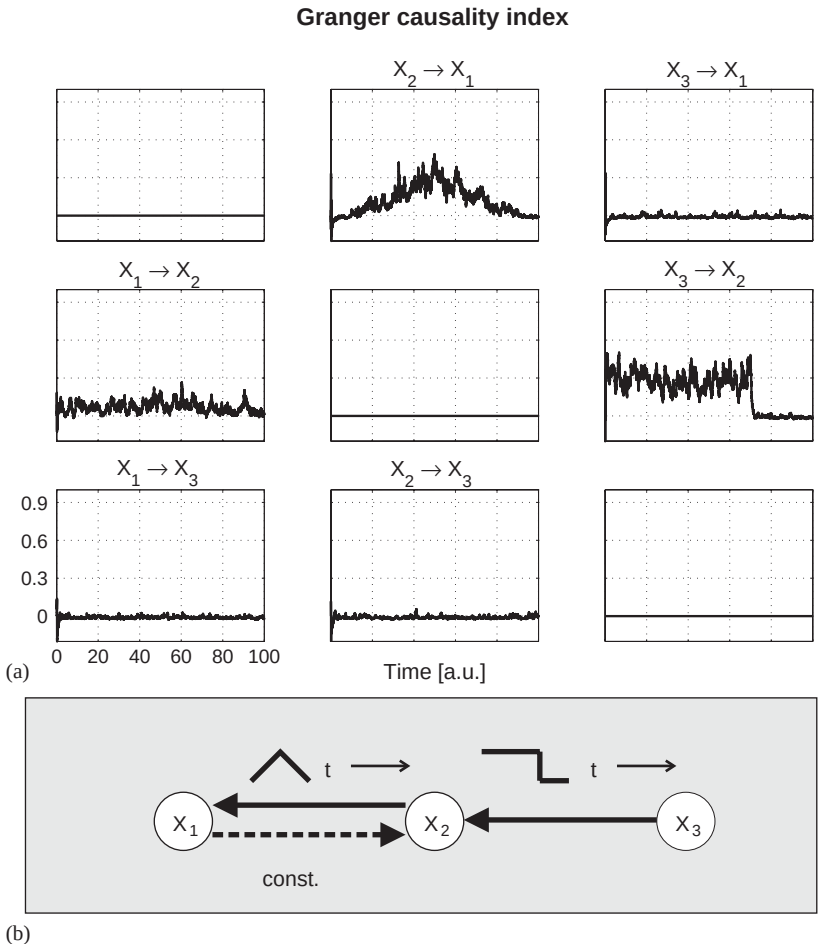

Fig. 10. Time-varying Granger causality index applied to the three-dimensional, time-varying VAR-model (a), which is summarized in the graph in (b). The influence from process X_1 to process X_2 is constant with time and is detected by a weak Granger causality index (dashed arrow). In contrast, the influence from process X_2 to process X_1 is not constant as indicated by the Granger causality index, but modulated by a triangular function. In addition, the abrupt change in the interrelation from process X_3 to X_2 is also detected correctly by the Granger causality index.

GABAergic input of reticular thalamic nucleus (RTN) activity induces inhibition of thalamo-cortical volley activity which is reflected by cortical interburst activity [44,45]. This in turn is assumed to be responsible for disconnection of afferent sensory input leading to unconsciousness [46]. The role of burst activity in terms of information transfer remains elusive. Therefore, we studied BSP in order to elaborate time and frequency-dependent features of information transfer between intrathalamic, thalamo-cortical and cortico-thalamic networks. Patterns were induced by propofol infusion in juvenile pigs and derived from cortical and thalamic electrodes. The analysis was performed to clarify a suggested time-dependent directed influence between the above mentioned brain structures known to be essentially involved in regulation of the physiological variation in consciousness during wakefulness and during sleep [32,47] as well as responsible to induce unconsciousness during administration of various anesthetic and sedative compounds [46]. In

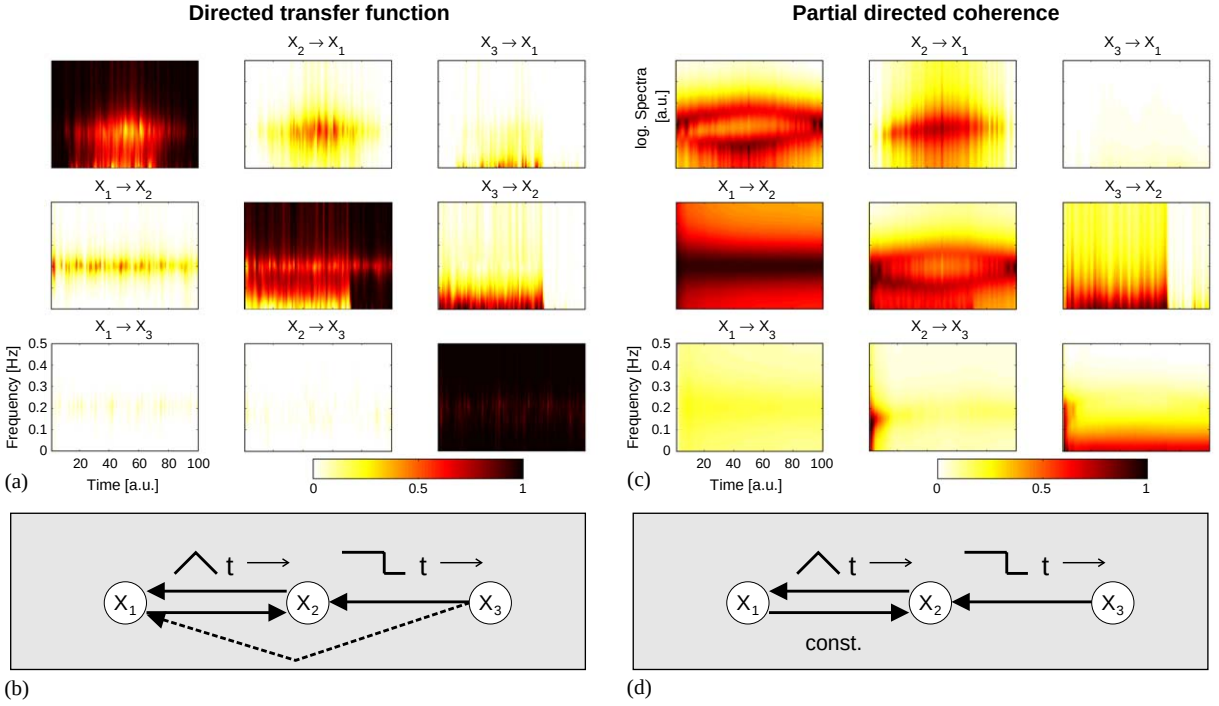

Fig. 11. Time-varying directed transfer function applied to a three-dimensional, time-varying VAR-model (a). On the diagonal the auto-directed transfer functions are shown. With the exception of the direct influence from process X_1 to X_2, from process X_2 to X_1, and from process X_3 to X_2, one indirect but directed interrelation is detected from X_3 to X_1, which is highest for those time points, where both influences from process X_3 to X_2 and X_2 to X_1 are highest. Compared to the Granger causality index, the functional relationship of the influences, especially for the triangular modulated influence, is more difficult to observe. However, the frequency dependence of the interrelations is easier to trace. The graph summarizing the results is shown in (b). The dashed arrow marks the indirect influence from process X_3 to process X_1. Corresponding results using time-varying partial directed coherence are shown in (c). On the diagonal the spectra of the processes are given. Compared to the directed transfer function approach results are very similar. The indirect influence from process X_3 to X_1 is unmasked by partial directed coherence. In contrast to the other approaches, the directed interrelation between X_1 and X_2 is rather large. This is caused by the fact that partial directed coherence is normalized by the influencing process. There is a spurious influence from process X_2 onto X_3 for the first few time units, which is caused by edge effects of the estimation procedure. The results are summarized in the graph in (d).

addition, the alternating occurrence pattern characteristic of burst activity allowed a triggered analysis of the GCI. Multiple trials enable to use a generalized recursive least square estimator [14,30], providing a more stable VAR parameter estimation and a calculation of a significance level based on these repetitions.

4.1. Experimental protocol and data acquisition

The investigation was carried out on six female, domestic juvenile pigs (mixed breed, 7 weeks old, 15.1 ± 1.4 kg b.w). Deep sedation with BSP was induced by continuous propofol infusion. Initially, 0.9 mg/kg b.w./min of propofol for approximately 7 min were administered until occurrence of BSP in occipital leads [31], followed by a maintenance dose of 0.36 mg/kg b.w./min. Ten screw electrodes at frontal, parietal, central, temporal, and occipital brain regions were utilized for ECoG recordings. For signal analysis a recording from the left parietooccipital cortex (POC) was used. Electrodes introduced stereotactically into the rostral part of the RTN and the dorsolateral thalamic nucleus (LD) of the left side were used for the electrothalamogram (EThG) recordings (cf. Fig. 12a).

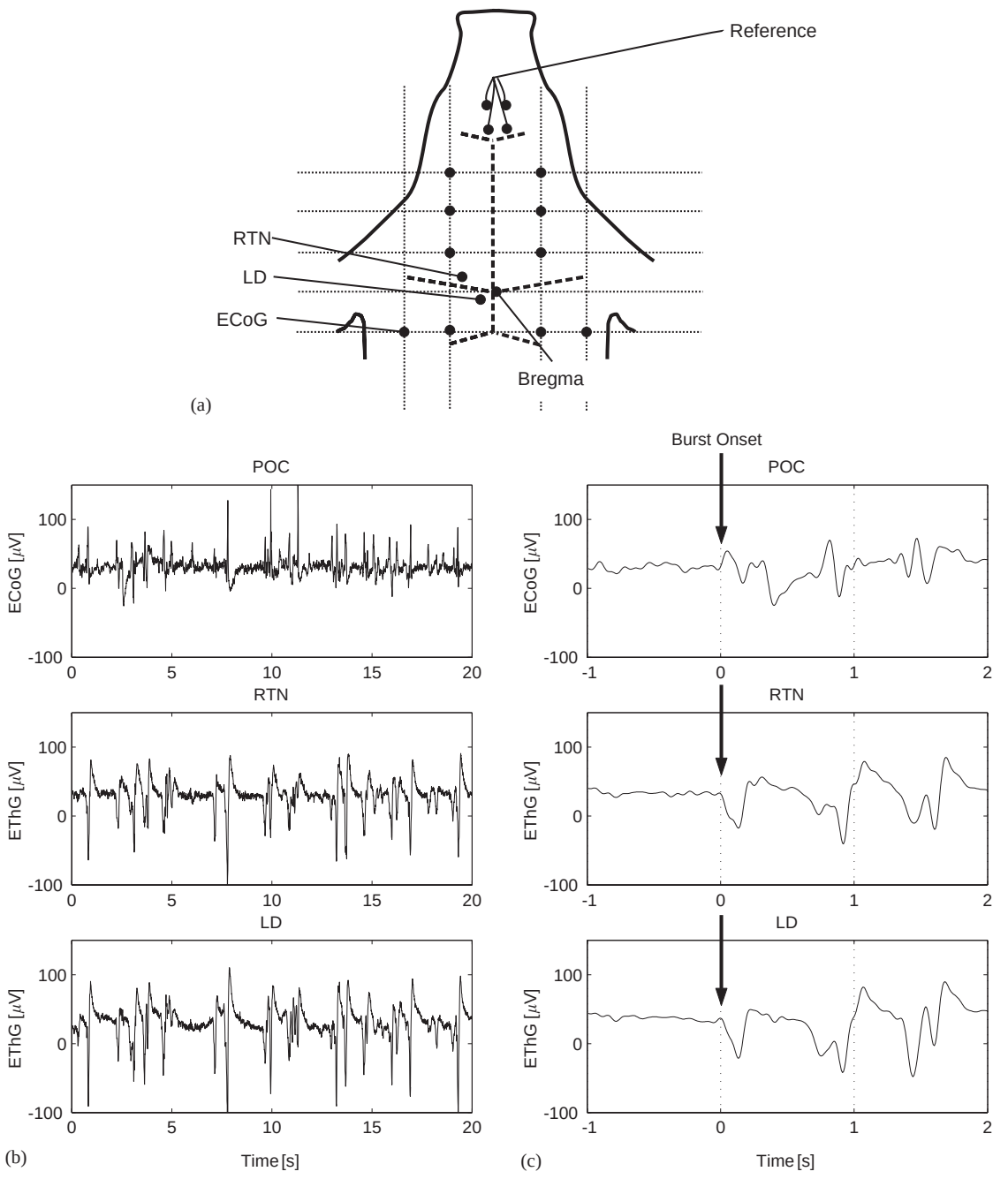

Fig. 12. (a) Schematic representation of electrode localizations. ECoG indicates POC recording which is used in the present investigation. Additionally, the RTN recording and LD recording were utilized. (b) 20 s section of continuous original trace and (c) one representative trial of triggered original traces of brain electrical activity simultaneously recorded from cortical and thalamic structures of a juvenile pig under propofol-induced deep sedation.

Unipolar signals were amplified and filtered (12-channel DC, 0.5–1000 Hz bandpass filter, 50 Hz notch filter; Fa. Schwind, Erlangen) before sampled continuously (125 Hz) with a digital data acquisition system (GJB Datentechnik GmbH, Langewiesen). Four linked screw electrodes inserted into the nasal bone served as reference. ECoG and EThG recordings were checked visually to exclude artifacts.

4.2. Analysis of time-variant and multivariate causal influences within distinct thalamo-cortical networks

In order to quantify time-variant and multivariate causal influences in a distinct functional state of general brain activity, we have chosen a representative example of deep sedation, characterized by existence of BSP. We used registrations from both thalamic leads (LD, RTN) and from the POC, which is known to respond early with patterns typical for gradual sedation including BSP [31]. In the present application, results for the GCI and the PDC are discussed, since a time-resolved extension of partial coherence is not considered and the DTF approach leads to results similar to PDC.

For PDC analysis continuous registrations of 384 s duration were utilized to provide an overview of the entire recording (Fig. 12b). For a closer investigation of the burst patterns the analysis using the GCI was applied to triggered registrations of 3 s duration each, i.e. 1 s before and 2 s after burst onset (Fig. 12c). In a total of 66 trials, trigger points were identified by visual inspection and were set at the burst onset. The deep sedation state was characterized by a distinct BSP in the POC lead as well as continuous high amplitude and low frequency activity in both thalamic leads.

For the entire time series of 384 s duration, pairwise PDC analysis was performed to investigate time-varying changes in directed influences between both thalamic structures RTN and LD and the POC. The results are shown in Fig. 13(a). On the diagonal the time-resolved auto-spectra are given. The graph summarizing the influences is given in Fig. 13(b). A strong and continuous influence is observed from both thalamic leads RTN and LD to POC at approximately 2 Hz. For the opposite direction, the causal influences are restricted to the low frequency range (<1 Hz) indicated by the dashed arrows in the graph. Furthermore, a directed influence is strongly indicated between the thalamic leads from LD to RTN, while the opposite direction shows a tendency to lower frequencies. The time-dependency is more pronounced in the interaction between both thalamic leads.

A clearer depiction of the interrelation structures occurring during the single burst patterns is presented in Fig. 14 by applying the GCI to segments of 3 s duration. For pairwise analysis between the three signals (cf. Fig. 14a and b), directed influences from both thalamic leads to the POC are observed for broad time periods. At several, well-defined time points, causal influences are detected for the opposite direction and between both thalamic leads (dashed arrows). The interrelation between the thalamic leads remains significant for the multivariate analysis given in Fig. 14(c) and (d). The directed influence from POC to LD and RTN is reduced to the burst onsets. From RTN and LD to the POC, no significant interrelation is traceable.

Results from the multivariate GCI cannot be directly correlated to the results obtained by the bivariate analysis. In particular, the missing interrelation from RTN and LD to POC is difficult to interpret with the knowledge of the bivariate results. One possible explanation might be an additional but unobserved process commonly influencing the three processes. This assumption is suggested by the results obtained from somatosensory-evoked potential (SEP) analysis (Fig. 15). In contrast to previous opinions of a proposed functional disconnection of afferent sensory inputs to thalamo-cortical networks during interburst periods leading to a functional state of unconsciousness [46], SEP analysis indicates that even during this particular functional state a signal transduction appears from peripheral skin sensors via thalamo-cortical networks up to cortical structures leading to signal processing. Hence in principle, a subthalamic generated continuous input could be responsible for the pronounced influence in the low frequency band, as shown by

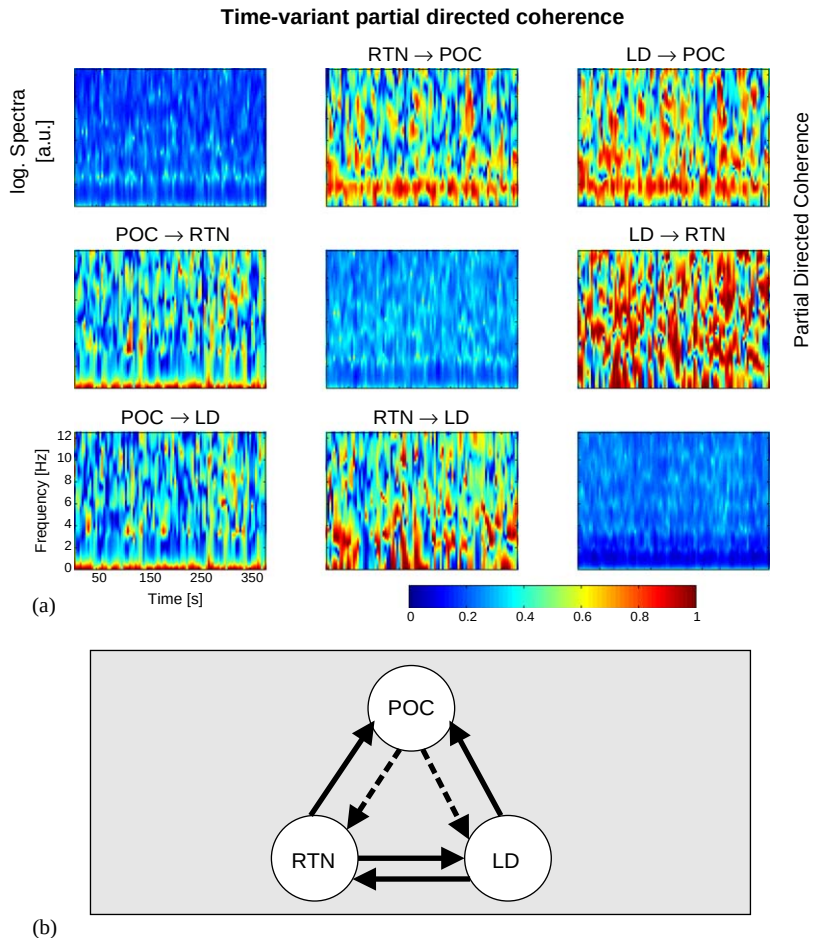

Fig. 13. Pairwise partial directed coherence based on state-space modeling for the signals of 384 s duration (a). On the diagonal the spectra are shown. Partial directed coherences from the thalamic leads RTN and LD to POC indicate a pronounced influence at approximately 2 Hz. The opposite direction is restricted to low frequencies (< 1 Hz). Both thalamic leads are mutually influencing each other. The graph summarizing the results is shown in (b). The dashed arrows correspond to influences for low frequencies.

PDC analysis. Such a low frequency component might not be observable by the GCI due to the missing selectivity for specific frequency bands.

Problems in the estimation procedure caused by, for instance, highly correlated processes or missing of important processes could also explain this effect [15]. Furthermore, the discrepancies between the bivariate and multivariate analysis could be due to the nonlinear behavior of the system. However, we claim that this possibility is not very likely, because spectral properties obtained in PDC analysis do not indicate a highly nonlinear behavior.

5. Discussion of applicability of multivariate linear analysis techniques to neural signal transfer

In this study we investigated and compared the properties of linear multivariate time series analysis techniques, i.e. non-parametric cross-spectral and parametric approaches. In the application of these methods to neural signal transfer, for example in the analysis of neural coordination in either the normal or pathological brain, one should be aware not only of the potentials but also the limitations of the methods. For this purpose, the features of the different analysis

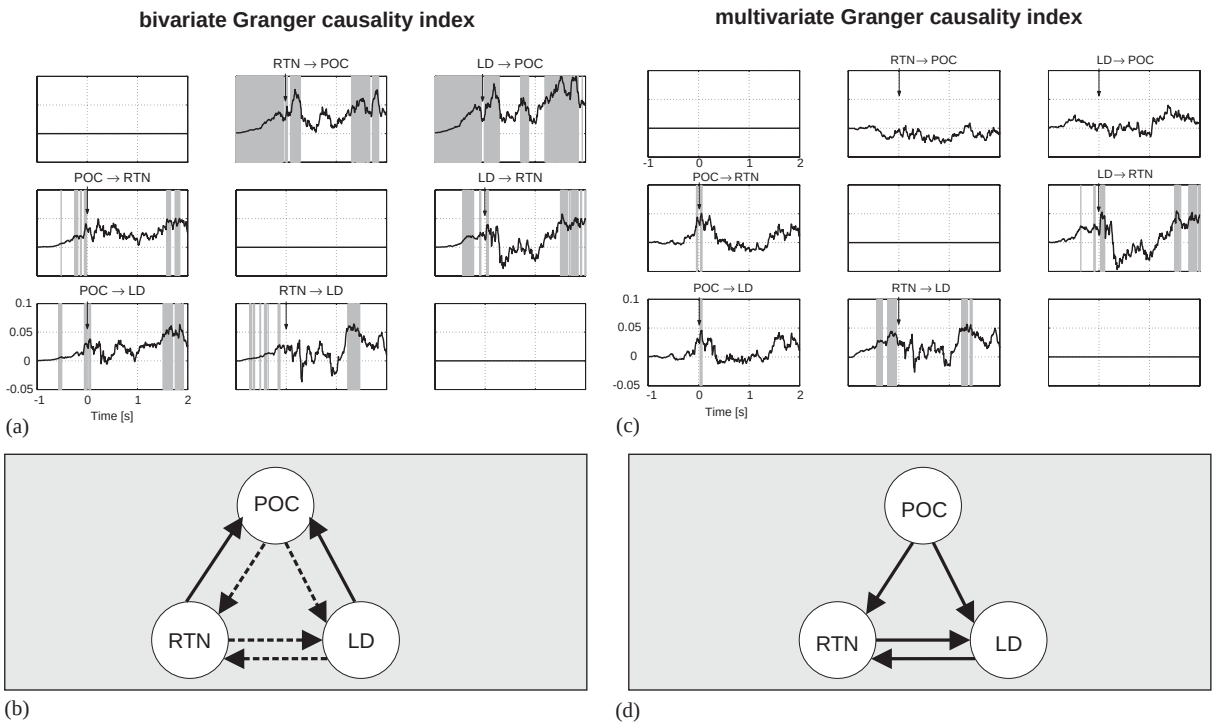

Fig. 14. Investigation of directed interrelations during the occurrence of burst patterns using the Granger causality index in the time-domain. Gray-colored regions indicate significant influences (alpha = 5%,one-sided). When applying pairwise analysis, directed influences from both thalamic leads LD and RTN to the parietooccipital cortex (POC) are detected (a). The results are summarized in the graph in (b). The dashed arrows corresponds to interactions lasting for short time intervals. The interrelation between the thalamic leads remains significant for the multivariate analysis (c). The directed influence from the parietooccipital cortex (POC) to the investigated thalamic structures is exclusively sustained at the burst onsets. The graph summarizing the results is given in (d).

techniques were analyzed by means of synthetic data simulated by various model systems.

To demonstrate the performance of the multivariate analysis techniques on a system they are developed for, a linear vector autoregressive model system was investigated first. In order to assess the specificity of the methods, independent noise processes with dramatically different variances were analyzed. Since it has not yet been fully determined whether particularly linear parametric methods can be applied to nonlinear systems, which are found in various fields of research, a multivariate Roessler system was examined. The Roessler system is a representative of the wide class of nonlinear chaotic systems. Finally, a time-variant and thus non-stationary system completed the investigation on model systems. Analysis techniques which do not account for such time dependence of interactions and processes themselves, reveal only averaged results of the true interrelation structure. Non-stationary data are in particular expected when investigating brain neural networks.

We note, however, that the simulations performed in this study cannot include the totality of the huge number and variety of multivariate systems. But this should not lessen the value of the comparison. To capture all reasonable situations, a countless number of systems and corresponding parameter choices would have to be investigated. However, the simulations presented here may be considered representative of the many situations faced in real-life applications. They are substantiated by at least heuristic arguments

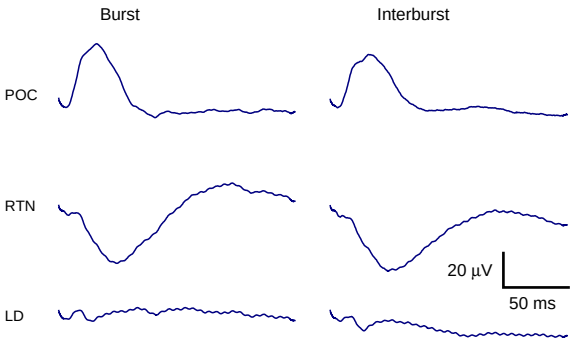

Fig. 15. Evoked activity derived from the parietooccipital cortex (POC, upper panel), rostral part of reticular thalamic nucleus thalamus (RTN, middle panel) and dorsolateral thalamic nucleus (LD, lower panel) owing to bipolar stimulation of the trigeminal nerve by a pair of hypodermic needles inserted on left side of the outer disc ridge of the porcine snout (rectangular pulses with constant current, duration of 70 μs, 1 Hz repetition frequency, 100 sweeps were averaged) in order to obtain somatosensory-evoked potentials (SEP) during burst as well as interburst periods. Note a similar signal pattern during burst and interburst periods.

Table 1
Summary of the results obtained by the comparison of the four multivariate time series analysis techniques

	PC	GCI	DTF	PDC
Direct versus indirect interactions	+	+	–	+
Direction of influences	(–)	+	+	+
Specificity in absence of influences	+	+	(+)	(+)
Nonlinearity of data	+	–	(+)	+
Influences varying with time	+	+	+	

To evaluate the performance, five aspects are considered. The brackets denote some specific limitations.

revealing reasons for the properties of the methods in various situations. For specific problems, simulations should be performed in advance of each analysis tailored to the investigated problem.

On the basis of the simulations, the performance of the four investigated analysis techniques, i.e. PC with its corresponding phase spectrum, the GCI, the DTF, and the PDC are summarized with respect to five aspects (cf. Table 1), which are important when analyzing brain neural networks:

- *Direct and indirect interactions*: A differentiation between direct and indirect information transfer in multivariate systems is not possible by means of the DTF. Therefore, the DTF is not sensitive in this sense (minus sign in Table 1). The remaining multivariate analysis techniques are in general able to distinguish between direct and indirect interactions. Thus, the GCI, PDC, and PC are sensitive in distinguishing direct from indirect influences. Despite the high sensitivity in general, there might be some situations in which this characteristic is restricted, for instance in nonlinear systems, nonstationary systems, etc.
- *Direction of influences*: All multivariate methods are capable of detecting the direction of influences. Partial coherence in combination with its phase spectrum is limited to high coherence values and to unidirectional influences between the processes. This shortcoming of partial coherence and partial phase spectrum is indicated by the minus sign in Table 1.
- *Specificity in absence of influences*: All four analysis techniques reject interrelations in the absence of any influence between the processes, reflecting the high specificity of the methods. For the parametric approaches DTF and PDC, a renormalization of the covariance matrix of the noise in the estimated VAR-model is required. Otherwise spurious interactions are detected. A significance level for both techniques should account for this. For the significance level for PDC, this dependence on the noise variance is explicitly considered. However, the renormalization is necessary to achieve a balanced average height of values of PDC and DTF in the case of an absence of an interaction at the corresponding frequency.
- *Nonlinearity of data*: For the nonlinear coupled stochastic Roessler system with pronounced frequencies, analysis techniques in the frequency domain are preferable. High model orders are required to describe the nonlinear system sufficiently with a linear VAR-model. As there is no analytical significance level, interpretation of the results obtained by the DTF and the GCI is more complicated. The PC, PDC, and the DTF are sensitive in detecting interactions in nonlinear multivariate systems. The GCI does not reveal the correct interrelation structure.

- *Influences varying with time*: In this study, partial coherence is not examined as a time-varying analysis technique. The GCI, DTF, and the time-varying PDC detect various types of time-varying influences. Therefore they are sensitive for time-resolved investigations of non-stationary data.

This summary provides an overview of which analysis techniques are appropriate for specific applications or problems. We note, however, that the particular capabilities and limitations of a specific analysis technique do not simply point to drawbacks of the method in general. If for instance the major task is to detect directions of influences, the DTF is applicable even if the differentiation, for example of direct or indirect interactions, is not possible.

Partial coherence as a non-parametric method is robust in detecting relationships in multivariate systems. Direct and indirect influences can be distinguished in linear systems and in the example of the nonlinear stochastic Roessler system. Since partial coherence is a non-parametric approach, it is possible to capture these influences without knowledge of the underlying dynamics. Furthermore, the statistical properties are well-known and critical values for a given significance level can be calculated in order to decide on significant influences. This is an important fact especially in applications to noisy neural signal transfer as measured by e.g. EEG recordings. A drawback is that the direction of relationships can only be determined by means of phase spectral analysis. If spectral coherence is weak or restricted to a small frequency range, directions of influences are difficult to infer by means of partial phase spectral analysis. Additionally, mutual interactions between two processes are also hardly detectable utilizing partial phase spectra.

Defined in the time-domain, the GCI is favorable in systems where neither specific frequencies nor frequency-bands are exposed in advance. The GCI utilizes information from the covariance matrix. Weak interactions or narrow-band interactions are difficult to detect since they lead to only small changes in the covariance matrix. This property accounts for the fact that when applying the GCI to the nonlinear signals of the coupled Roessler systems, the coupling scheme was no longer detectable. The GCI, estimated by means of the recursive least square algorithm, renders a methodology to trace interdependence structures in non-stationary data possible. This might become important in applications to brain neural networks, when the time course of transitions in neural coordination is of particular interest.

By means of the DTF, directions of influences in multivariate dynamical systems are detectable. Nevertheless, in contrast to the remaining three analysis techniques under investigation in the present study, a differentiation between indirect and direct influences is not possible using the DTF. Analyzing brain networks, at least weakly nonlinear processes might by expected to generate the neural signals. In the application to the nonlinear stochastic Roessler system, the directions of the couplings have been observed at the oscillation frequencies. The DTF benefits from its property as an analysis technique in the frequency domain. Increasing the order of the fitted model system is sufficient to capture the main features of the system and thus to detect the interdependence structure correctly. Nevertheless, a matrix inversion is required for estimating the DTF, which might lead to computational challenges especially if high model orders are necessary. In order to detect transitions in the coordination between neural signals, the DTF is useful when applying a time-resolved parameter estimation procedure.

In our investigations of synthetic data sets, PDC has been the most powerful analysis technique. By means of PDC, direct and indirect influences as well as their directions are detectable. The investigation of the paradigmatic model system of coupled stochastic Roessler oscillators has shown that at least for weak nonlinearities coupling directions can be inferred by means of PDC. Increasing the order of the fitted model is required to describe the nonlinear system by a linear VAR-model sufficiently. However, as the statistical properties of PDC and significance levels for the decision of significant influences are known, high model orders of the estimated VAR-model are less problematic. Using additionally time-resolved parameter estimation techniques, PDC is applicable to non-stationary

signals. Using this procedure, influences in dependence on time and frequency are simultaneously detectable. Since in applications to neural networks it is usually unknown whether there are changes in neural coordination or whether such changes are of particular interest, respectively, time-resolved analysis techniques avoid possible false interpretations.

The promising results showing that most parametric linear analysis techniques have revealed correct interaction structures in multivariate systems, indicates beneficial applicability to empirical data. We analyzed electrophysiological signals from thalamic and cortical brain structures representative for key interrelations within a network responsible for control and modulation of consciousness. We used data obtained from experimental recordings of deep sedation with BSP, which allows usage of data from a well-defined functional state including a triggered analysis approach. PDC based on state space modeling allows for inference of the time- and frequency-dependence of the interrelation structure. The mechanisms generating burst patterns were investigated in more detail by applying the GCI. Besides a clear depiction of the system generating such burst patterns, the application presented here demonstrates, that time dependence is not negligible.

In conclusion, several analysis techniques exist to detect interrelation structures in multivariate systems. We compared four different analysis techniques and described their different performances and properties. Since each analysis technique is superior for specific problems, simultaneous application of several analysis techniques is the preferable procedure.

Acknowledgments

The study was partly supported by the German Research Foundation DFG (Scha741/3-2, Ti315/2-1), by the Interdisciplinary Center of Clinical Research of the Medical Faculty, Friedrich Schiller University Jena, (Part 1.13, TMWF B 307-04004), and by the German Federal Ministry of Education and Research (BMBF-FKZ 01 ZZ 0105 and BMBF grant 01GQ0420).

References

[1] H. Witte, C. Schelenz, M. Specht, H. Jäger, P. Putsche, M. Arnold, L. Leistritz, K. Reinhart, Interrelations between EEG frequency components in sedated intensive care patients during burst-suppression period, Neurosci. Lett. 260 (1999) 53–56.

[2] M. Särkelä, S. Mustola, T. Seppänen, M. Koskinen, P. Lepola, K. Suominen, T. Juvonen, H. Tolvanen-Laakso, V. Jäntti, Automatic analysis and monitoring of burst suppression in anesthesia, J. Clin. Mon. Comp. 17 (2002) 125–134.

[3] M. Steriade, F. Amzica, D. Contreras, Cortical and thalamic cellular correlates of electroencephalographic burst-suppression, Electroenceph. Clin. Neurophysiol. 90 (1994) 1–16.

[4] M. Steriade, D. Contreras, R.C. Dossi, A. Nunez, The slow (less-than-1 Hz) oscillation in reticular thalamic and thalamocortical neurons—scenario of sleep rhythm generation in interacting thalamic and neocortical networks, J. Neurosci. 13 (1993) 3284–3299.

[5] M. Arnold, H. Witte, C. Schelenz, Time-variant investigation of quadratic phase couplings caused by amplitude modulation in electroencephalic burst-suppression patterns, J. Clin. Mon. Comput. 17 (2002) 115–123.

[6] J. Muthuswamy, D.L. Sherman, N.V. Thakor, Higher-order spectral analysis of burst patterns in EEG, IEEE Trans. Biomed. Eng. 46 (1999) 92–99.

[7] B. Schack, H. Witte, M. Helbig, C. Schelenz, M. Specht, Time-variant non-linear phase-coupling analysis of EEG burst patterns in sedated patients during electroencephalic burst suppression period, Clin. Neurophysiol. 112 (2001) 1388–1399.

[8] D.R. Brillinger, Time Series: Data Analysis and Theory, Holden-Day, Inc., San Francisco, 1981.

[9] D. Contreras, A. Destexhe, T.J. Sejnowski, M. Steriade, Spatiotemporal patterns of spindle oscillations in cortex and thalamus, J. Neurosci. 17 (1997) 1179–1196.

[10] R. Dahlhaus, Graphical interaction models for multivariate time series, Metrika 51 (2000) 157–172.

[11] J. Granger, Investigating causal relations by econometric models and cross-spectral methods, Econometrica 37 (1969) 424–438.

[12] M.J. Kamiński, K.J. Blinowska, A new method of the description of the information flow in the brain structures, Biol. Cybern. 65 (1991) 203–210.

[13] L.A. Baccala, K. Sameshima, Partial directed coherence: a new concept in neural structure determination, Biol. Cybern. 84 (2001) 463–474.

[14] W. Hesse, E. Möller, M. Arnold, B. Schack, The use of time-variant EEG Granger causality for inspecting directed interdependencies of neural assemblies, J Neurosci. Methods 124 (2003) 27–44.

[15] B. Schelter, B. Hellwig, B. Guschlbauer, C.H. Lücking, J. Timmer, Application of graphical models in bilateral essential tremor, Proc. IFMBE (EMBEC) 2 (2002) 1442–1443.

[16] R. Dahlhaus, M. Eichler, J. Sandkühler, Identification of synaptic connections in neural ensembles by graphical models, J. Neurosci. Methods 77 (1997) 93–107.
[17] M. Eichler, R. Dahlhaus, J. Sandkühler, Partial correlation analysis for the identification of synaptic connections, Biol. Cybern. 89 (2003) 289–302.
[18] J.R. Rosenberg, D.M. Halliday, P. Breeze, B.A. Conway, Identification of patterns of neuronal connectivity–partial spectra, partial coherence, and neuronal interactions, J. Neurosci. Methods 83 (1998) 57–72.
[19] S. Boccaletti, J. Kurths, G. Osipov, D.L. Valladares, C.S. Zhou, The synchronization of chaotic systems, Phys. Rep. 366 (2002) 1–101.
[20] A. Pikovsky, M. Rosenblum, J. Kurths, Synchronization—A Universal Concept in Nonlinear Sciences, Cambridge University Press, Cambridge, 2001.
[21] P. Tass, M.G. Rosenblum, J. Weule, J. Kurths, A. Pikovsky, J. Volkmann, A. Schnitzler, H.J. Freund, Detection of n:m phase locking from noisy data: application to magnetoencephalography, Phys. Rev. Lett. 81 (1998) 3291–3295.
[22] F. Varela, J.P. Lachaux, E. Rodriguez, J. Martinerie, The brain web: phase synchronization and large-scale integration, Nat. Rev. Neurosci. 2 (2001) 229–239.
[23] B. Pompe, P. Blidh, D. Hoyer, M. Eiselt, Using mutual information to measure coupling in the cardiorespiratory system, IEEE Eng. Med. Biol. 17 (1998) 32–39.
[24] L.A. Baccala, K. Sameshima, G. Ballester, A.C. Valle, C. Timo-Iaria, Studying the interaction between brain structures via directed coherence and Granger causality, Appl. Signal Process. 5 (1998) 40–48.
[25] L.A. Baccala, K. Sameshima, Overcoming the limitations of correlation analysis for many simultaneously processed neural structures, Prog. Brain Res. 130 (2001) 33–47.
[26] E.E. Fanselow, K. Sameshima, L.A. Baccala, M.A.L. Nicolelis, Thalamic bursting in rats during different awake behavioral states, Proc. Natl. Acad. Sci. 98 (2001) 15330–15335.
[27] M.J. Kamiński, K.J. Blinowska, W. Szelenberger, Topographic analysis of coherence and propagation of EEG activity during sleep and wakefulness, Electroencephalogr. Clin. Neurophysiol. 102 (1997) 216–227.
[28] M.J. Kamiński, M. Ding, W.A. Truccolo, S.L. Bressler, Evaluating causal relations in neural systems: Granger causality directed transfer function and statistical assessment of significance, Biol. Cybern. 85 (2001) 145–157.
[29] R. Kus, M. Kamiński, K.J. Blinowska, Determination of EEG activity propagation: pair-wise versus multichannel estimate, IEEE Trans. Biomed. Eng. 51 (2004) 1501–1510.
[30] E. Möller, B. Schack, M. Arnold, H. Witte, Instantaneous multivariate EEG coherence analysis by means of adaptive high-dimensional autoregressive models, J Neurosci. Methods 105 (2001) 143–158.
[31] E. Niedermeyer, D.L. Sherman, R.J. Geocadin, H.C. Hansen, D.F. Hanley, The burst-suppression electroencephalogram, Clin. Electroencephalogr. 30 (1999) 99–105.
[32] E.F. Pace-Schott, J.A. Hobson, The neurobiology of sleep: genetics, cellular physiology and subcortical networks, Nat. Rev. Neurosci. 3 (2002) 591–605.
[33] O.E. Rössler, An equation for continuous chaos, Phys. Lett. A 57 (1976) 397–398.
[34] K. Sameshima, L.A. Baccala, Using partial directed coherence to describe neuronal ensemble interactions, J. Neurosci. Methods 94 (1999) 93–103.
[35] J. Timmer, M. Lauk, S. Häußler, V. Radt, B. Köster, B. Hellwig, B. Guschlbauer, C.H. Lücking, M. Eichler, G. Deuschl, Cross-spectral analysis of tremor time series, Int. J. Bif. Chaos 10 (2000) 2595–2610.
[36] P. Bloomfield, Fourier Analysis of Time Series: An Introduction, Wiley, New York, 1976.
[37] P.J. Brockwell, R.A. Davis, Time Series: Theory and Methods, Springer, New York, 1993.
[38] B. Schelter, M. Winterhalder, M. Eichler, M. Peifer, B. Hellwig, B. Guschlbauer, C.H. Lücking, R. Dahlhaus, J. Timmer, Testing for directed influences in neuroscience using partial directed coherence, Preprint Series DFG-SPP 1114, 2005, pp. 73.
[39] A.C. Harvey, Forecasting Structural Time Series Models and the Kalman Filter, Cambridge University Press, Cambridge, 1994.
[40] R.H. Shumway, D.S. Stoffer, Time Series Analysis and its Application, Springer, New York, 2000.
[41] B. Schelter, M. Winterhalder, K. Schwab, L. Leistritz, W. Hesse, R. Bauer, H. Witte, J. Timmer, Quantification of directed signal transfer within neural networks by partial directed coherence: a novel approach to infer causal time-depending influences in noisy, multivariate time series, Preprint Series DFG-SPP 1114, 2005, pp. 70.
[42] R. Dahlhaus, M. Eichler, Causality and Graphical Models for time series, in: P. Green, N. Hjort, S. Richardson (Eds.), Highly Structured Stochastic Systems, Oxford University Press, Oxford, 2003.
[43] J. Timmer, What can be inferred from surrogate data testing?, Phys. Rev. Lett. 85 (2000) 2647.
[44] E.G. Jones, Thalamic circuitry and thalamocortical synchrony, Philos. Trans. R. Soc. Lond. B. Biol. Sci. 357 (2002) 1659–1673.
[45] M. Steriade, Impact of network activities on neuronal properties in corticothalamic systems, J. Neurophysiol. 86 (2001) 1–39.
[46] M.T. Alkire, R.J. Haier, J.H. Fallon, Toward a unified theory of narcosis: brain imaging evidence for a thalamocortical switch as the neurophysiologic basis of anesthetic-induced unconsciousness, Conscious Cogn. 9 (2000) 370–386.
[47] J.A. Hobson, E.F. Pace-Schott, The cognitive neuroscience of sleep: neuronal systems, consciousness and learning, Nat. Rev. Neurosci. 3 (2002) 679–693.